Mode Atlas for the TESLA 1.3 GHz Structure

W. Ackermann, H. De Gersem, C. Liu, T. Weiland
Institut für Theorie Elektromagnetischer Felder, Technische Universität Darmstadt

TECHNISCHE UNIVERSITÄT DARMSTADT

Outline

TECHNISCHE UNIVERSITÄT DARMSTADT

- Motivation
- Computational model
  - Geometry information concerning the cavity and the couplers (number and location of ports)
  - Numerical problem formulation
- Numerical examples
  - 1.3 GHz structure (single cavity)

    Summary of all modes up to the 5th dipole passband
- Summary / Outlook

Outline

TECHNISCHE UNIVERSITÄT DARMSTADT

- Motivation
- Computational model
  - Geometry information concerning the cavity and the couplers (number and location of ports)
  - Numerical problem formulation
- Numerical examples
  - 1.3 GHz structure (single cavity)

    Summary of all modes up to the 5th dipole passband
- Summary / Outlook

Motivation

TECHNISCHE UNIVERSITÄT DARMSTADT

- TESLA 1.3 GHz Cavity
  - Photograph

http://newsline.linearcollider.org

  - Numerical model

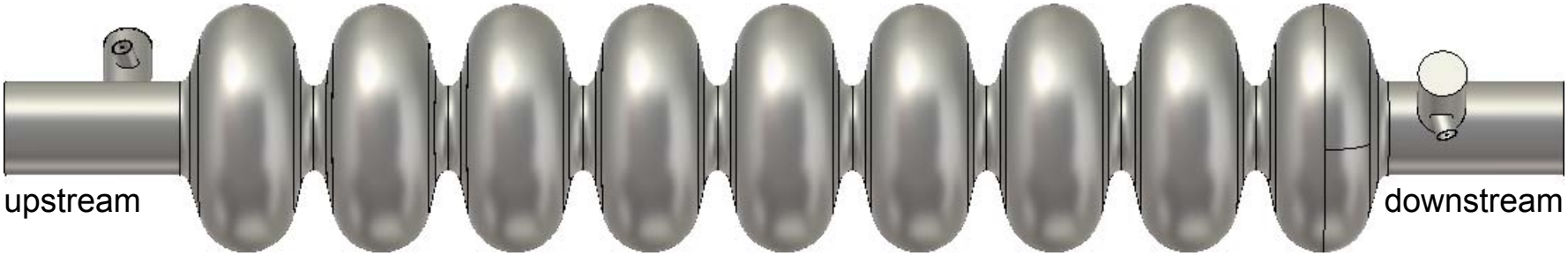

CST Studio Suite 2015

Motivation

TECHNISCHE UNIVERSITÄT DARMSTADT

- Superconducting resonator

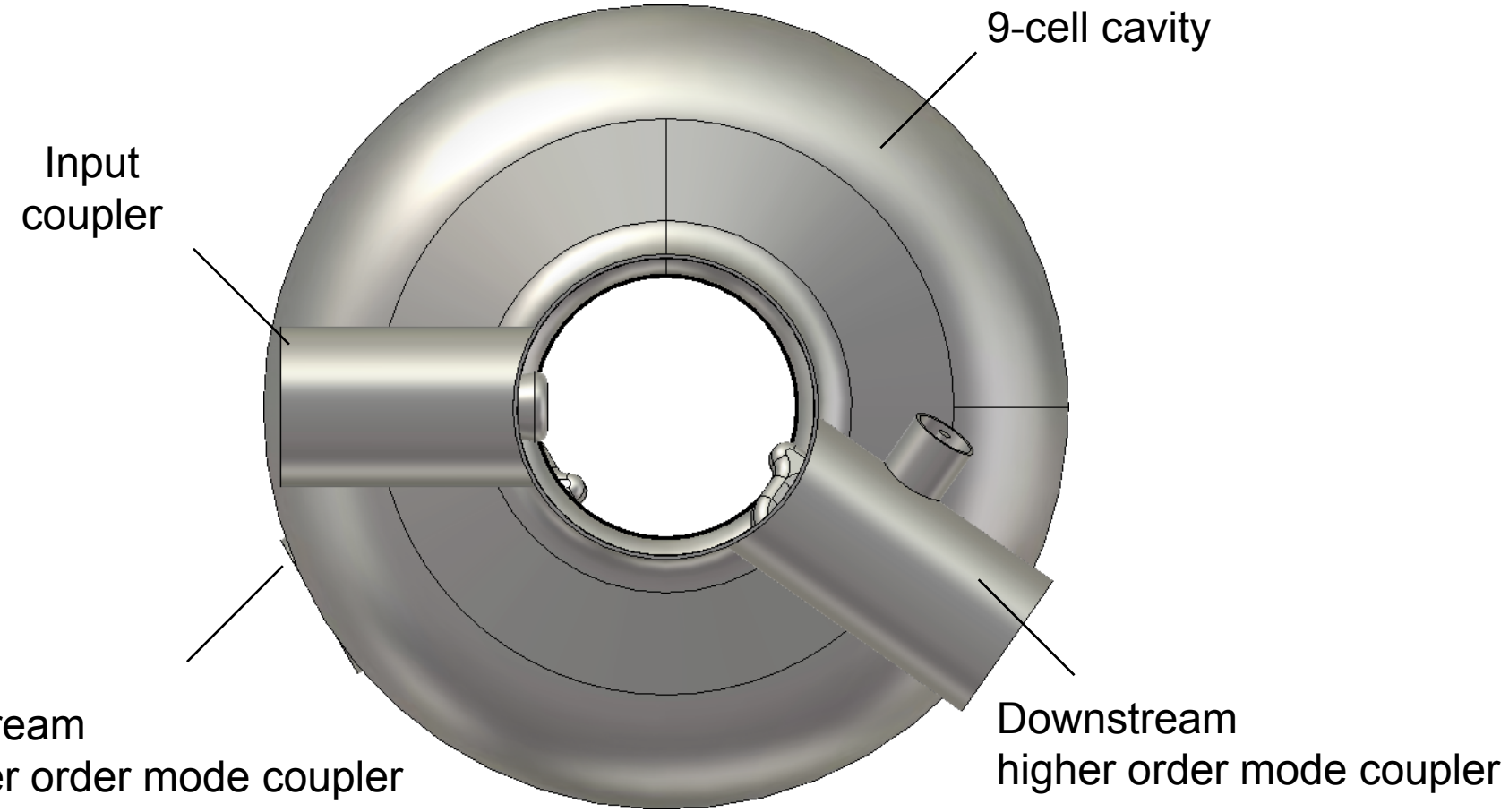

Motivation

TECHNISCHE UNIVERSITÄT DARMSTADT

- Simulation study based on 2D structures available

  Rainer Wanzenberg,
  TESLA 2001-33

  - Monopole, dipole and quadrupole modes of a TESLA cavity
  - “Obtained data intended to be used in further beam dynamics studies and in the interpretation of HOM measurements” (f, R/Q, …)

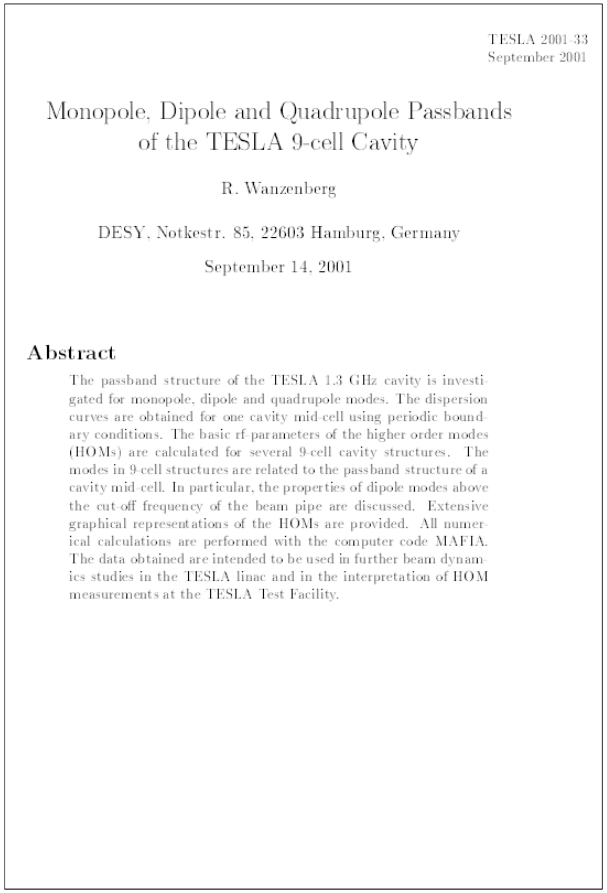

TESLA 2001-33
September 2001

Monopole, Dipole and Quadrupole Passbands of the TESLA 9-cell Cavity

R. Wanzenberg

DESY, Notkestr. 85, 22603 Hamburg, Germany

September 14, 2001

Abstract

The passband structure of the TESLA 1.3 GHz cavity is investigated for monopole, dipole and quadrupole modes. The dispersion curves are obtained for one cavity mid-cell using periodic boundary conditions. The basic rf parameters of the higher order modes (HOMs) are calculated for several 9-cell cavity structures. The modes in 9-cell structures are related to the passband structure of a cavity mid-cell. In particular, the properties of dipole modes above the cut-off frequency of the beam pipe are discussed. Extensive graphical representations of the HOMs are provided. All numerical calculations are performed with the computer code MAFIA. The data obtained are intended to be used in further beam dynamics studies in the TESLA linac and in the interpretation of HOM measurements at the TESLA Test Facility.

➡ Simulation study based on 3D structures using port boundary conditions (Q, R)

Outline

TECHNISCHE UNIVERSITÄT DARMSTADT

- Motivation
- Computational model
  - Geometry information concerning the cavity and the couplers (number and location of ports)
  - Numerical problem formulation
- Numerical examples
  - 1.3 GHz structure (single cavity)

    Summary of all modes up to the 5th dipole passband
- Summary / Outlook

Computational Model

TECHNISCHE UNIVERSITÄT DARMSTADT

- Geometrical model

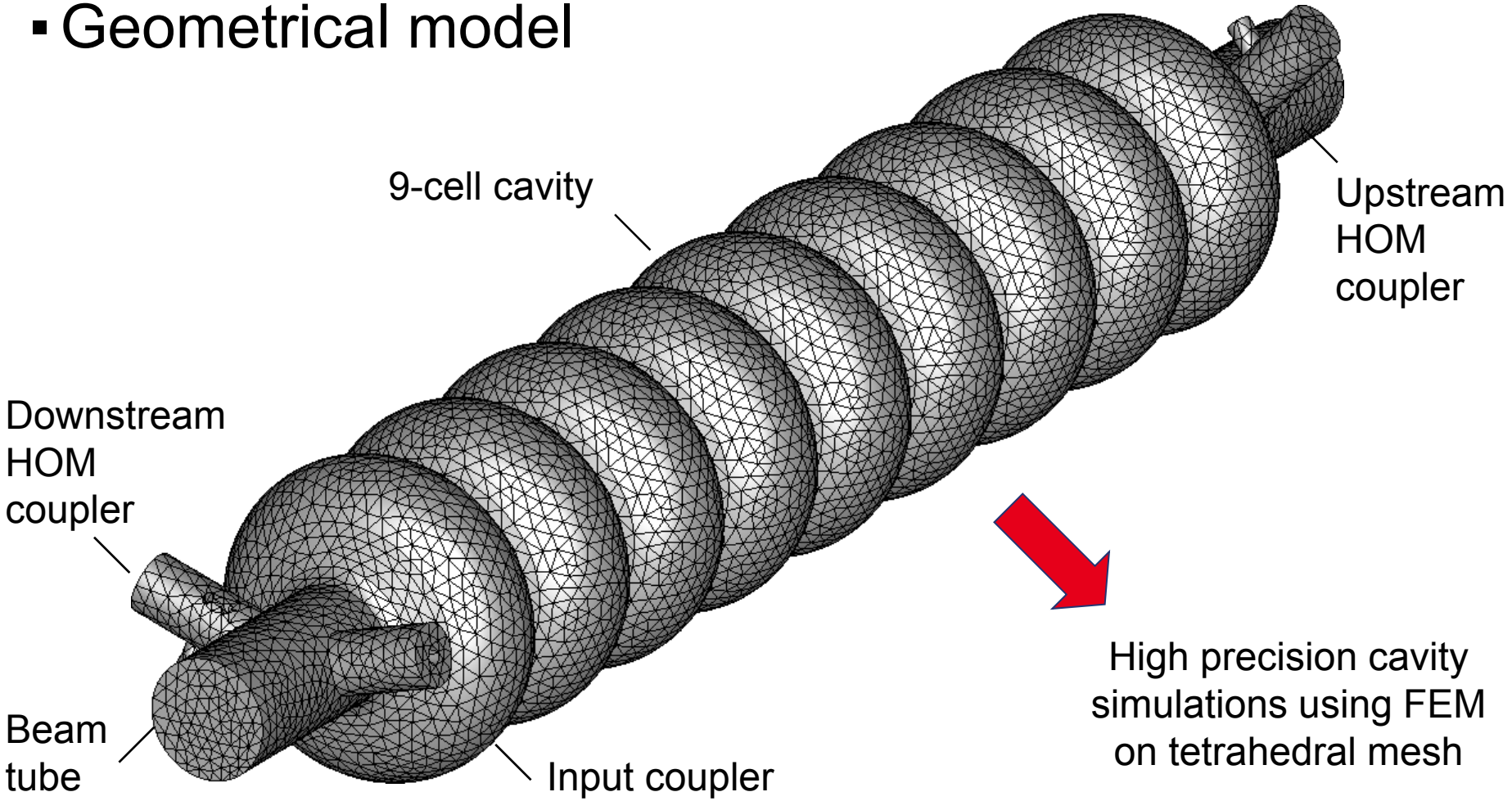

Computational Model

TECHNISCHE UNIVERSITÄT DARMSTADT

- Port boundary condition

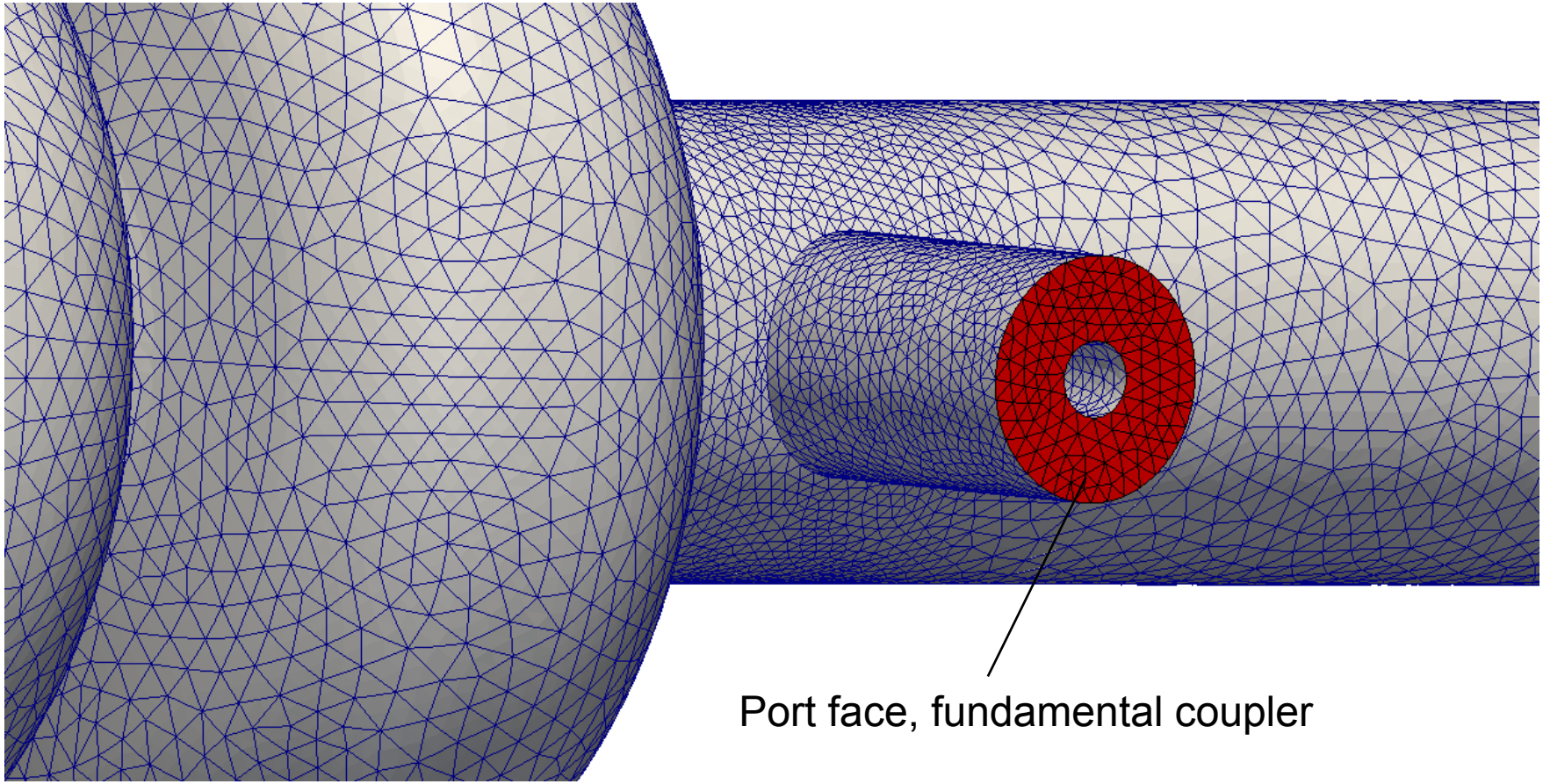

Computational Model

TECHNISCHE UNIVERSITÄT DARMSTADT

- Port boundary condition

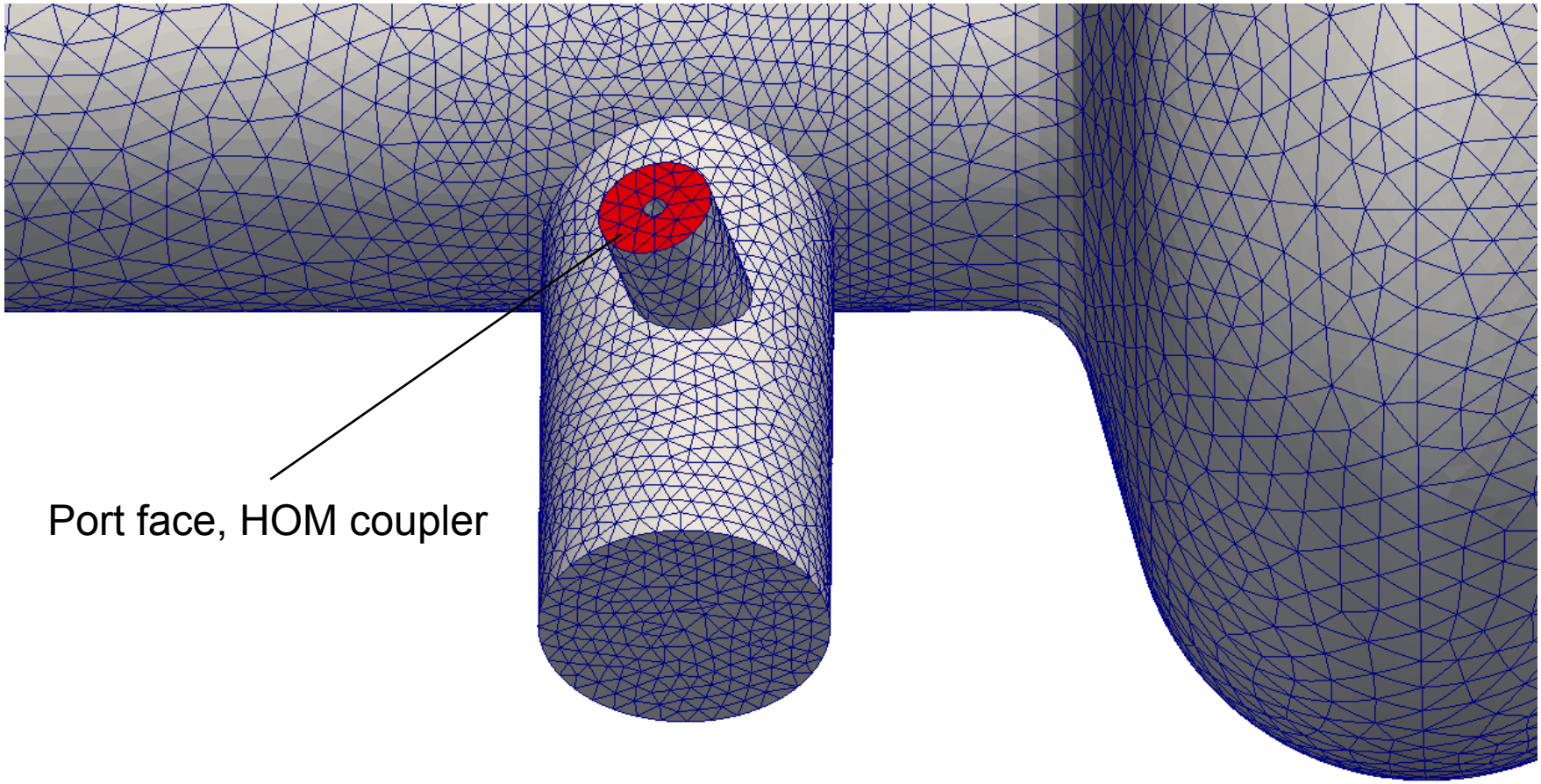

Computational Model

TECHNISCHE UNIVERSITÄT DARMSTADT

- Problem definition
  - Geometry

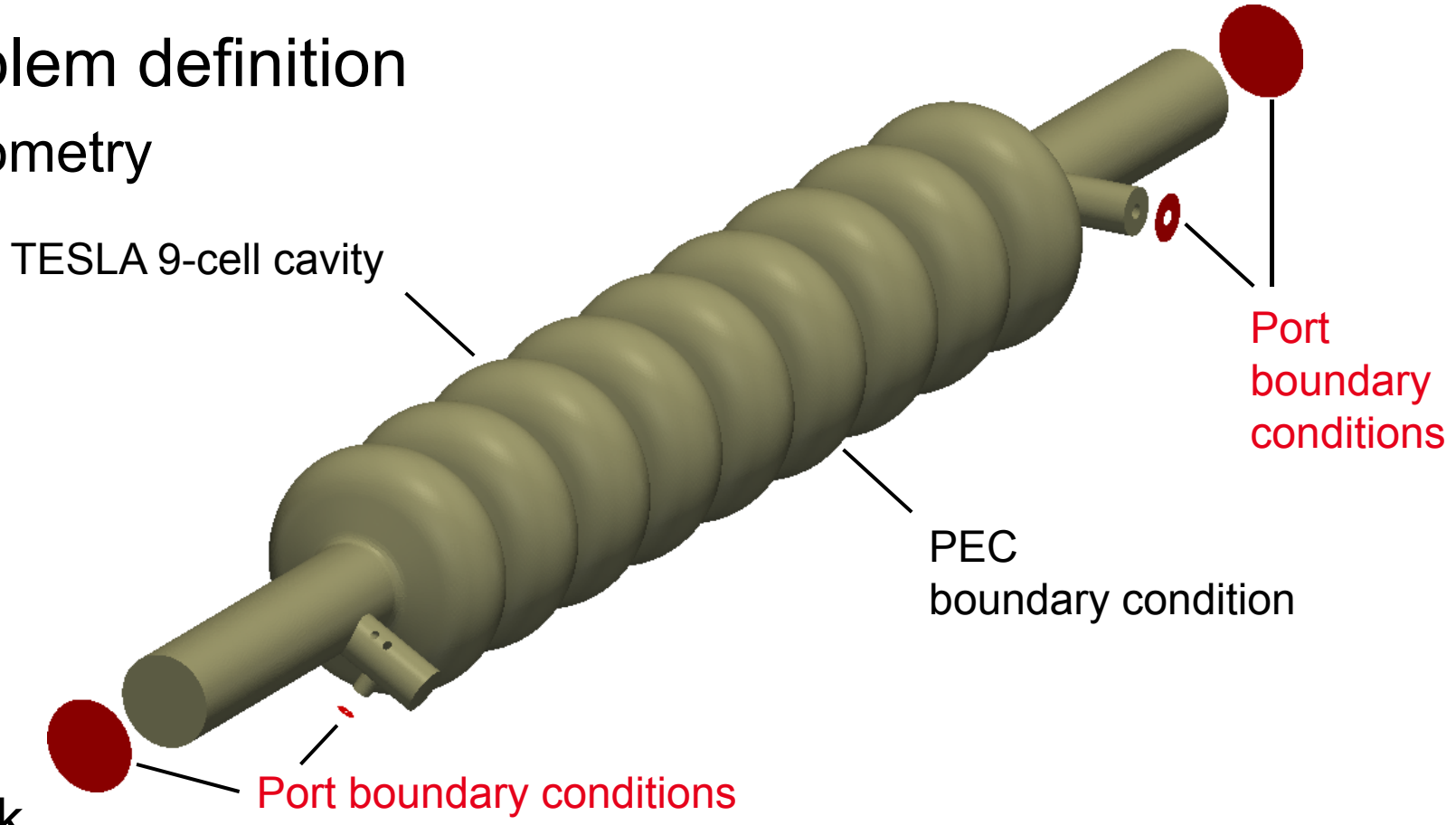

  - Task

    Search for the field distribution, resonance frequency and quality factor

Computational Model

TECHNISCHE UNIVERSITÄT DARMSTADT

- Main Coupler Penetration Depth

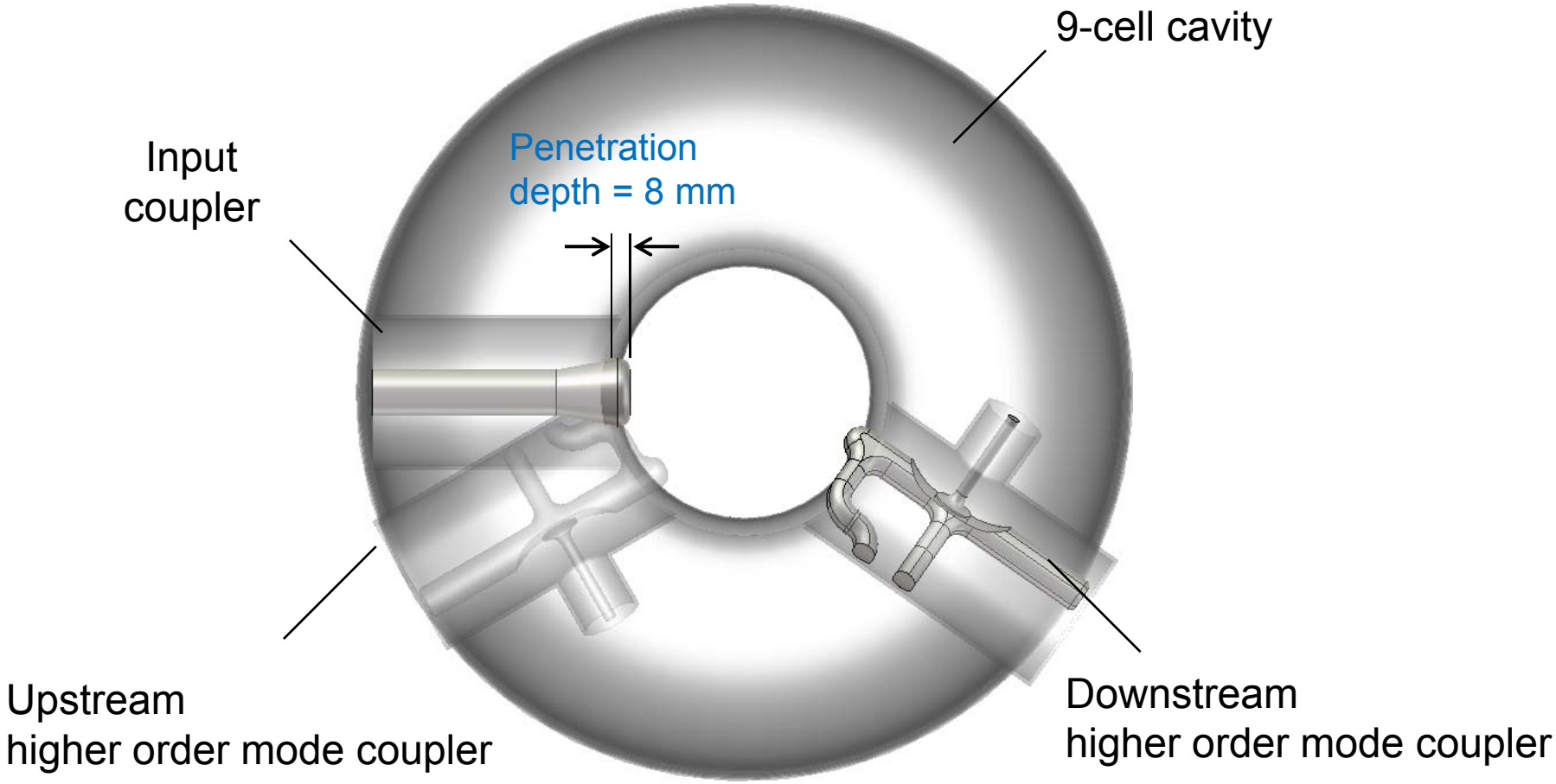

Computational Model

TECHNISCHE UNIVERSITÄT DARMSTADT

- Problem formulation
  - Local Ritz approach

$$\vec{E} = \vec{E}(\vec{r}) = \sum_{i=1}^{n} \alpha_i \, \vec{w}_i(\vec{r})$$

$\vec{w}$ vectorial function

α_i scalar coefficient

i global index

n number of DOFs

$$\operatorname{curl} 1/\mu_r \operatorname{curl}\vec{E} = \left(\frac{\omega}{c_0}\right)^2 \varepsilon_r \vec{E}\,\Big|_{\vec{r}\in\Omega}$$

$$\operatorname{div}(\varepsilon\vec{E})\Big|_{\vec{r}\in\Omega} = 0 \qquad \text{+ boundary conditions}$$

continuous eigenvalue problem

Galerkin

$$A_{ij} = \iiint_\Omega 1/\mu_r \operatorname{curl}\vec{w}_i \cdot \operatorname{curl}\vec{w}_j \, d\Omega$$

$$B_{ij} = \iiint_\Omega \varepsilon_r \, \vec{w}_i \cdot \vec{w}_j \, d\Omega$$

$$C_{ij} = \iiint_\Omega Z_0 \, \sigma \, \vec{w}_i \cdot \vec{w}_j \, d\Omega$$

$$A\vec{\alpha} + j\frac{\omega}{c_0} C\vec{\alpha} + (j\frac{\omega}{c_0})^2 B\vec{\alpha} = 0$$

discrete eigenvalue problem

Computational Model

TECHNISCHE UNIVERSITÄT DARMSTADT

- Eigenvalue calculation
  - Improved search space expansion
    - Davidson:

$$(A_{\text{diag}} - \lambda B_{\text{diag}})\Delta\vec{x} = -\vec{r}$$

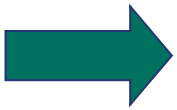

works well for diagonal dominant matrices

    - Jacobi-Davidson:

$$P^T(A - \lambda B)P\Delta\vec{x} = -P^T\vec{r}$$

correction equation

with

$$P = I - VV^TB = I - VV_B^T$$
$$P^T = I - BVV^T = I - V_BV^T$$

due to projection also applicable to non-diagonal dominant matrices

Computational Model

TECHNISCHE UNIVERSITÄT DARMSTADT

- Jacobi-Davidson method
  - Important properties
    - Direct solution difficult because of dense matrix in correction equation.
    - Iterative solution not immediately applicable because vectors $\Delta\vec{x}$ with $\Delta\vec{x} \in R\{(V_B)_\perp\}$ are not mapped back onto $R\{(V_B)_\perp\}$ again.
  - Preconditioning
    - The JD - preconditioner

$$PC = \{I - M^{-1}V_B[(M^{-1}V_B)^T V_B]^{-1}V_B^T\}M^{-1}$$
$$= M^{-1} - M^{-1}V_B[(M^{-1}V_B)^T V_B]^{-1}V_B^T M^{-1}$$

retains the property $\Delta\vec{x} \in R\{(V_B)_\perp\}$ for any preconditioner M^{-1}.

Simplest case: $M^{-1} = I \quad \hookrightarrow \quad PC = I - VV_B^T = P$

Outline

TECHNISCHE UNIVERSITÄT DARMSTADT

- Motivation
- Computational model
  - Geometry information concerning the cavity and the couplers (number and location of ports)
  - Numerical problem formulation
- Numerical examples
  - 1.3 GHz structure (single cavity)

    Summary of all modes up to the 5th dipole passband
- Summary / Outlook

Numerical Examples

TECHNISCHE UNIVERSITÄT DARMSTADT

- Controlling the Jacobi-Davidson eigenvalue solver
  - Evaluation in the complex frequency plane
  - Select best suited eigenvalues in circular region around user-specified complex target

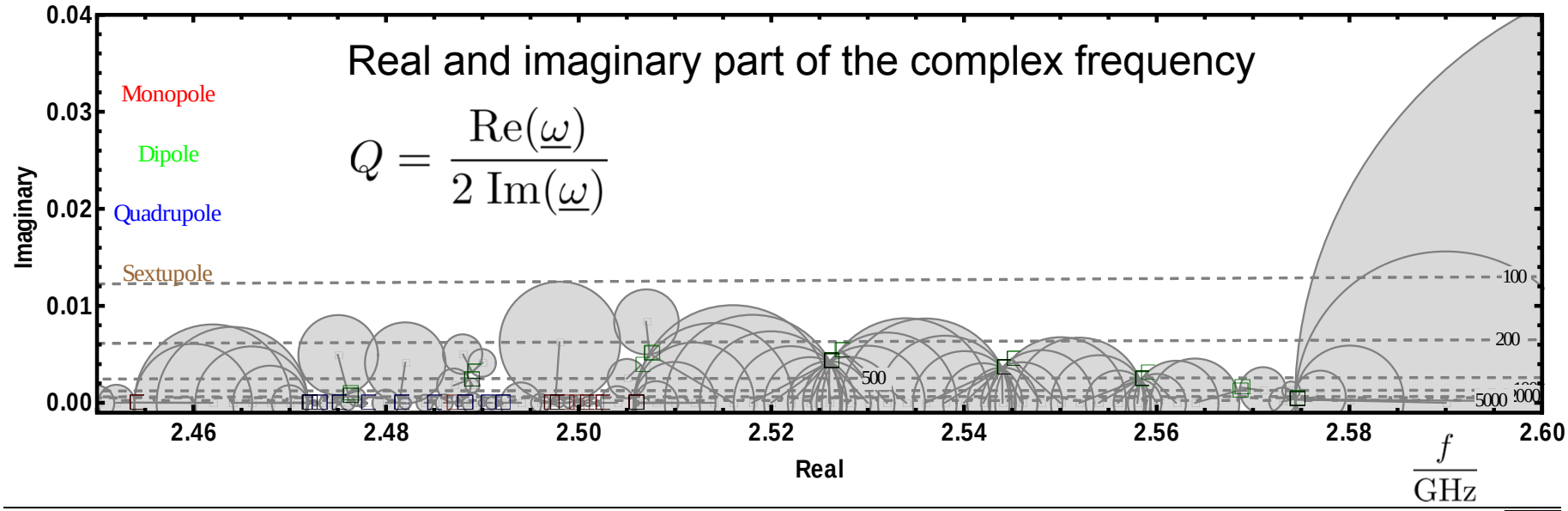

Numerical Examples

TECHNISCHE UNIVERSITÄT DARMSTADT

- Quality factor versus frequency

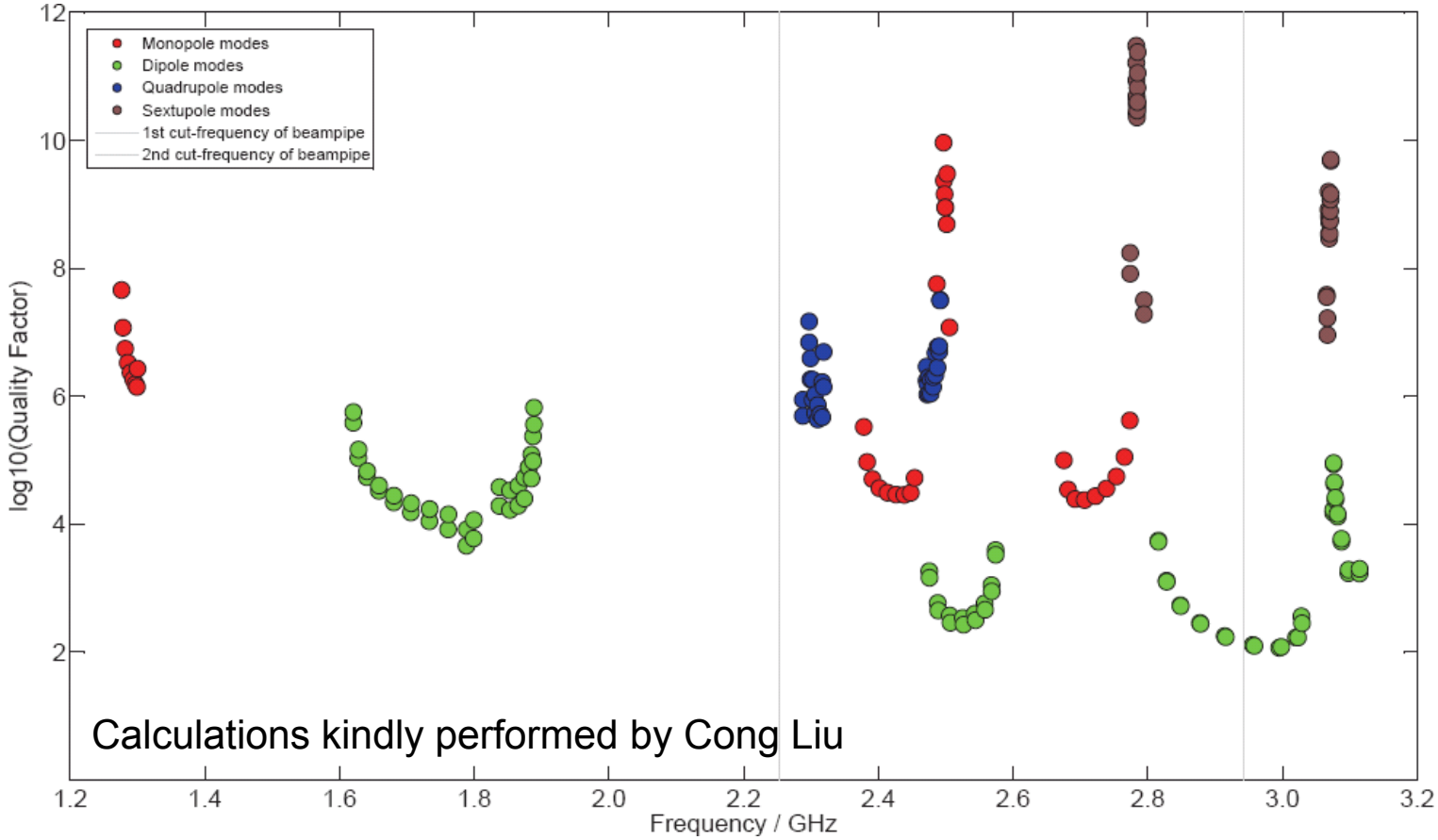

Numerical Examples

TECHNISCHE UNIVERSITÄT DARMSTADT

- Shunt Impedance Calculations
  - Longitudinal Voltage

$$V_{||}^{(m)}(x,y) = \int_{z_a}^{z_b} \vec{e}_z \cdot \vec{E}^{(m)}(x,y,z)\, e^{-j\omega/c\, z}\, \mathrm{d}z$$

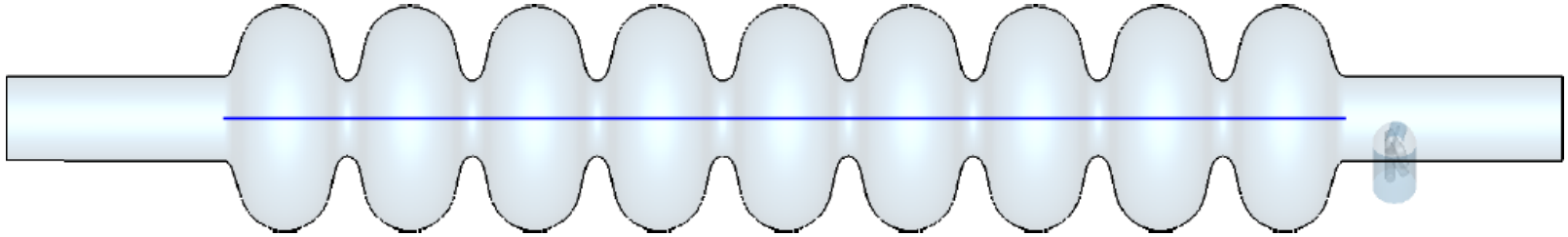

  - Stored Energy and Loss Parameter

$$U^{(m)} = \frac{\varepsilon_0}{2} \iiint_{\Omega} \varepsilon_r\, |\vec{E}^{(m)}|^2\, \mathrm{d}\Omega \qquad k_{||}^{(m)}(x,y) = \frac{|V_{||}^{(m)}(x,y)|^2}{4\, U^{(m)}}$$

Numerical Examples

TECHNISCHE UNIVERSITÄT DARMSTADT

- Shunt Impedance Calculations
  - Normalized Shunt Impedance

$$\frac{R^{(m)}}{Q} = \frac{2\, k_{||}^{(m)}(x,y)}{\omega\, (x^2+y^2)^m}$$

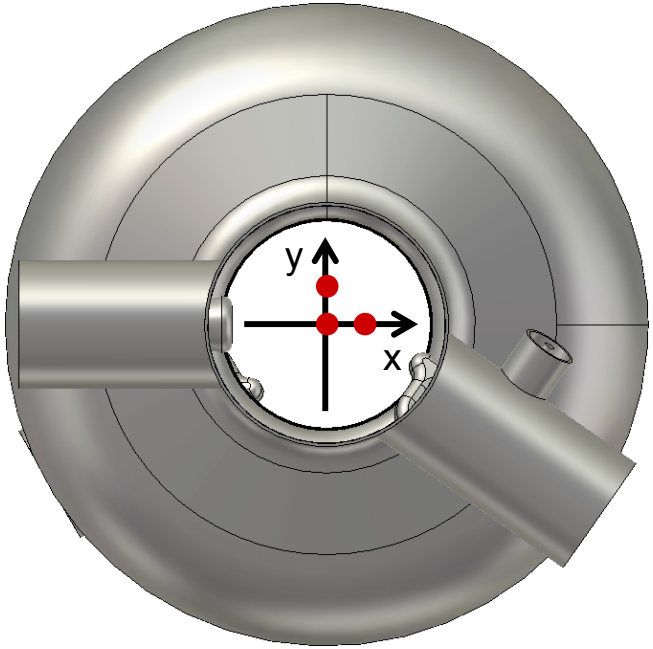

  - Evaluation of the integral at lines parallel to the z-axis

$$x_0 = 5\ \mathrm{mm}$$
$$y_0 = 5\ \mathrm{mm}$$

$$\frac{R_{\mathrm{x}}^{(m)}}{Q} = \frac{2\, k_{||}^{(m)}(x_0,0)}{\omega \quad x_0^{2m}}, \qquad \frac{R_{\mathrm{y}}^{(m)}}{Q} = \frac{2\, k_{||}^{(m)}(0,y_0)}{\omega \quad y_0^{2m}}, \qquad \frac{R_{\mathrm{z}}^{(m)}}{Q} = \frac{2\, k_{||}^{(m)}(0,0)}{\omega}$$

Numerical Examples

TECHNISCHE UNIVERSITÄT DARMSTADT

- Simulation study based on mesh density variations

- Grid 1

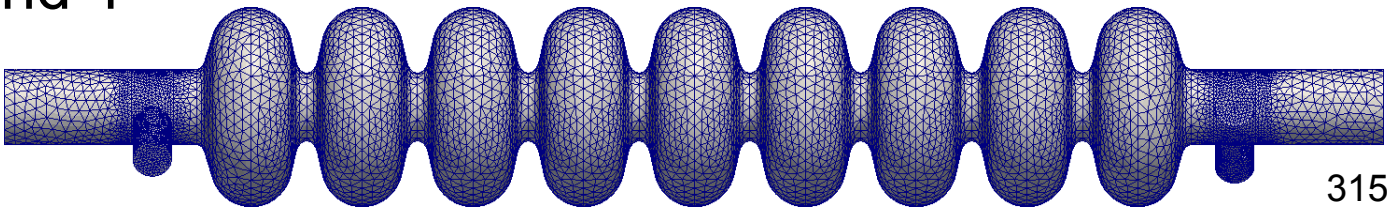

315.885 tetrahedrons
1.932.746 complex DOF

- Grid 2

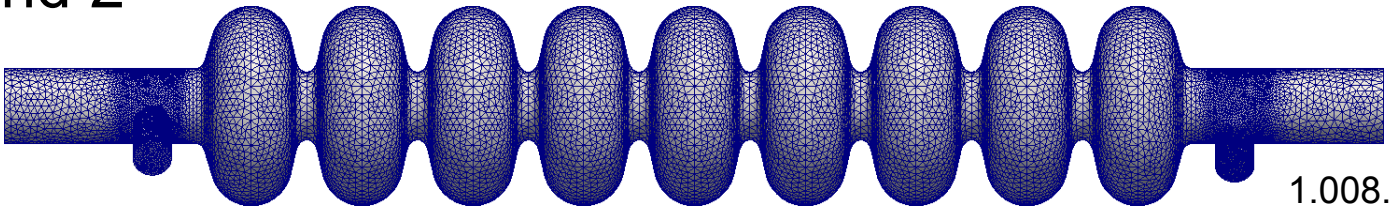

1.008.189 tetrahedrons
6.238.328 complex DOF

- Grid 3

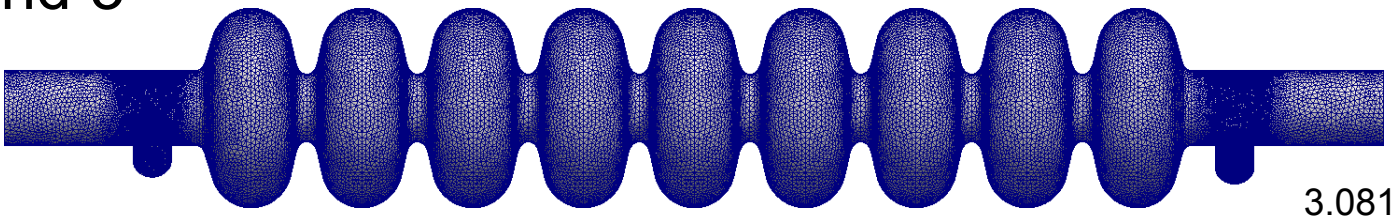

3.081.614 tetrahedrons
19.177.820 complex DOF

Numerical Examples

TECHNISCHE UNIVERSITÄT DARMSTADT

- Simulation study based on mesh density variations

Table 2: Monopole modes in 1st, 2nd, 3rd and 4th passband.

	fres (GHz)			Q		
MODE i	GRID 1	GRID 2	GRID 3	GRID 1	GRID 2	GRID 3
Band 1						
1	1.2763	1.2763	1.2764	4.63E+07	4.54E+07	4.52E+07
2	1.2784	1.2784	1.2784	1.20E+07	1.17E+07	1.16E+07
3	1.2816	1.2816	1.2816	5.58E+06	5.47E+06	5.43E+06
4	1.2855	1.2856	1.2856	3.38E+06	3.31E+06	3.28E+06
5	1.2898	1.2898	1.2898	2.37E+06	2.32E+06	2.30E+06
6	1.2938	1.2938	1.2938	1.85E+06	1.81E+06	1.80E+06
7	1.2971	1.2971	1.2971	1.57E+06	1.54E+06	1.52E+06
8	1.2993	1.2993	1.2993	1.41E+06	1.39E+06	1.37E+06
9	1.3000	1.3000	1.3000	2.79E+06	2.68E+06	2.65E+06
Band 2						
1	2.3784	2.3785	2.3786	3.33E+05	3.28E+05	3.21E+05
2	2.3833	2.3834	2.3835	9.45E+04	9.28E+04	9.09E+04
3	2.3912	2.3912	2.3913	5.09E+04	5.01E+04	4.91E+04
4	2.4015	2.4016	2.4016	3.66E+04	3.62E+04	3.55E+04
5	2.4136	2.4137	2.4137	3.09E+04	3.08E+04	3.03E+04
6	2.4265	2.4265	2.4265	2.87E+04	2.88E+04	2.84E+04
7	2.4386	2.4386	2.4386	2.83E+04	2.85E+04	2.82E+04
8	2.4483	2.4483	2.4482	3.06E+04	3.08E+04	3.05E+04
9	2.4539	2.4540	2.4539	5.27E+04	5.27E+04	5.21E+04
Band 3						
1	2.4869	2.4868	2.4868	4.64E+07	4.16E+07	5.01E+07
2	2.4969	2.4969	2.4969	1.11E+08	1.30E+10	1.33E+10
3	2.4976	2.4975	2.4975	2.29E+08	3.32E+09	2.83E+09
4	2.4985	2.4984	2.4984	4.64E+08	2.37E+09	2.01E+09
5	2.4995	2.4995	2.4995	3.87E+07	1.37E+09	1.27E+09
6	2.5006	2.5006	2.5006	2.01E+08	6.04E+08	1.45E+09
7	2.5016	2.5015	2.5015	1.48E+08	3.04E+08	1.48E+09
8	2.5022	2.5022	2.5021	2.82E+08	2.87E+09	4.68E+09
9	2.5057	2.5057	2.5057	1.55E+07	1.11E+07	1.28E+07
Band 4						
1	2.6755	2.6755	2.6756	9.99E+04	1.00E+05	9.95E+04
2	2.6817	2.6817	2.6818	3.47E+04	3.48E+04	3.46E+04
3	2.6922	2.6923	2.6923	2.46E+04	2.47E+04	2.46E+04
4	2.7063	2.7063	2.7064	2.38E+04	2.39E+04	2.39E+04
5	2.7224	2.7224	2.7224	2.73E+04	2.74E+04	2.74E+04
6	2.7387	2.7387	2.7387	3.60E+04	3.60E+04	3.59E+04
7	2.7536	2.7536	2.7536	5.58E+04	5.56E+04	5.54E+04
8	2.7657	2.7657	2.7657	1.13E+05	1.12E+05	1.12E+05
9	2.7735	2.7735	2.7735	4.23E+05	4.19E+05	4.15E+05

Band 1

Band 2

Band 3

Band 4

Individual pages available for

- f_{res}, Q
- R_x/Q, R_x
- R_y/Q, R_y
- R_z/Q, R_z

Grid 1 = 315.885 tetrahedrons
Grid 2 = 1.008.189 tetrahedrons
Grid 3 = 3.081.614 tetrahedrons

Numerical Examples

TECHNISCHE UNIVERSITÄT DARMSTADT

- Collection of the first 194 modes (selected page)

1. MONOPOLE PASSBAND

MODE 9

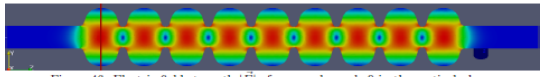

Figure 46: Electric field strength $|\vec{E}|$ of monopole mode 9 in the vertical plane.

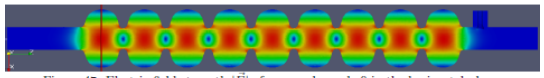

Figure 47: Electric field strength $|\vec{E}|$ of monopole mode 9 in the horizontal plane.

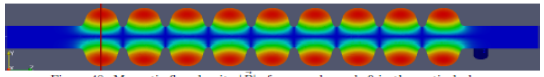

Figure 48: Magnetic flux density $|\vec{B}|$ of monopole mode 9 in the vertical plane.

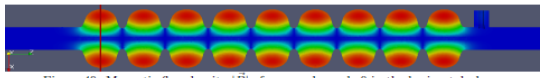

Figure 49: Magnetic flux density $|\vec{B}|$ of monopole mode 9 in the horizontal plane.

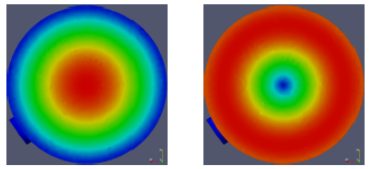

(a) Electric field strength $|\vec{E}|$ (b) Magnetic flux density $|\vec{B}|$

Figure 50: Absolute value of the electric field strength and the magnetic flux density of monopole mode 9 in a transverse plane indicated by a red line in the upper cut views.

Table 34: Characteristic values

Resonance frequency	fres	1.3000 GHz
Quality factor	Q	2.64e+006
Normalized transverse shunt impedance	$R_x^{(0)}/Q$	5.20e+002 Ω
Transverse shunt impedance	$R_x^{(0)}$	1.37e+009 Ω
Normalized transverse shunt impedance	$R_y^{(0)}/Q$	5.20e+002 Ω
Transverse shunt impedance	$R_y^{(0)}$	1.37e+009 Ω
Normalized longitudinal shunt impedance	$R_z^{(0)}/Q$	5.20e+002 Ω
Longitudinal shunt impedance	$R_z^{(0)}$	1.37e+009 Ω

Magnitude of the electric field strength (longitudinal cut)

Magnitude of the magnetic flux density (longitudinal cut)

Magnitude of the electric field and the magnetic flux density (transverse cut)

Resonance frequency, quality factor and shunt impedances

Numerical Examples

TECHNISCHE UNIVERSITÄT DARMSTADT

- Comparison to MAFIA calculations (f_{res} monopole)

Mode Index	1	2	3
1	1.276	1.276	1.276
2	1.278	1.278	1.278
3	1.282	1.282	1.282
4	1.286	1.286	1.286
5	1.290	1.290	1.290
6	1.294	1.294	1.294
7	1.297	1.297	1.297
8	1.299	1.299	1.299
9	1.300	1.300	1.300
10	2.378	2.379	2.379
11	2.383	2.383	2.383
12	2.391	2.391	2.391
13	2.402	2.402	2.402
14	2.414	2.414	2.414
15	2.426	2.426	2.426
16	2.439	2.439	2.439
17	2.448	2.448	2.448
18	2.454	2.454	2.454
19	2.487	2.487	2.487
20	2.497	2.497	2.497
21	2.498	2.498	2.498
22	2.498	2.498	2.498
23	2.500	2.499	2.499
24	2.501	2.501	2.501
25	2.502	2.502	2.502
26	2.502	2.502	2.502
27	2.506	2.506	2.506

Mode Index	1	
1	1.276	
2	1.278	
3	1.281	
4	1.285	
5	1.289	
6	1.292	
7	1.296	
8	1.298	
9	1.298	
10	2.380	
11	2.386	
12	2.394	
13	2.406	
14	2.418	
15	2.431	
16	2.442	
17	2.450	
18	2.454	
19	-----	TE modes
20	-----	
21	-----	
22	-----	
23	-----	
24	-----	
25	-----	
26	-----	
27	-----	

MAFIA:
step size 1mm
12.000 grid points

Reference: (TESLA 2001-33)
Monopole, Dipole and Quadrupole
Passbands of the TESLA 9-cell Cavity,
R. Wanzenberg, September 14, 2001

Different monopole passband numbering!

Outline

TECHNISCHE UNIVERSITÄT DARMSTADT

- Motivation
- Computational model
  - Geometry information concerning the cavity and the couplers (number and location of ports)
  - Numerical problem formulation
- Numerical examples
  - 1.3 GHz structure (single cavity)

    Summary of all modes up to the 5th dipole passband
- Summary / Outlook

Summary / Outlook

TECHNISCHE UNIVERSITÄT DARMSTADT

- Summary:

  Accurate complex eigenmode solver available

  - Higher order FEM including port boundary conditions (geometric modeling with curved 2D and 3D elements)
  - Application to the 1.3 GHz structure (calculation of all modes up the 5th dipole passband)
  - Quality factor and field polarizations intrinsically available

- Outlook:

  - Application and further development of the available code

Outlook

TECHNISCHE UNIVERSITÄT DARMSTADT

- Application of the available eigenvalue solver
  - PETRA cavities
    - PMC, PEC and port boundary conditions sufficient?
    - Apply power-loss method to consider lossy metal effects?
    - Surface impedance boundary condition (SIBC) required?
- Further eigenvalue-solver development
  - Implement SIBC
  - Increase computational efficiency
    - Replace LU based preconditioner by numerically cheaper variant